



| | |
|--------------------|--|
| Title | General analysis on the use of tesla's resonators in domino forms for wireless power transfer |
| Author(s) | Zhong, Wenxing; Lee, Chi Kwan; Ron Hui, S. Y. |
| Citation | IEEE Transactions on Industrial Electronics, 2013, v. 60, n. 1, p. 261-270 |
| Issued Date | 2013 |
| URL | http://hdl.handle.net/10722/225038 |
| Rights | This work is licensed under a Creative Commons Attribution-NonCommercial-NoDerivatives 4.0 International License. |

General Analysis on the Use of Tesla's Resonators in Domino Forms for Wireless Power Transfer

Wenxing Zhong, Chi Kwan Lee, *Member, IEEE*, and S. Y. Ron Hui, *Fellow, IEEE*

Abstract—In this paper, we present a brief overview of historical developments of wireless power and an analysis on the use of Tesla's resonators in domino forms for wireless power transfer. Relay resonators are spaced between the transmitter and receiver coils with the objectives of maximizing energy efficiency and increasing the overall transmission distance between the power source and the load. Analytical expressions for the optimal load and maximum efficiency at resonance frequency are derived. These equations are verified with practical measurements obtained from both coaxial and noncoaxial domino resonator systems. To avoid the use of high operating frequency for wireless power transfer in previous related research, the technique presented here can be used at submegahertz operation so as to minimize the power loss in both the power supply and the output stage. We demonstrated both theoretically and practically that unequal spacing for the coaxial straight domino systems has better efficiency performance than the equal-spacing method. Also, the flexibility of using resonators in various domino forms is demonstrated.

Index Terms—Domino resonator system, maximum efficiency operation, relay resonator, wireless power transfer (WPT).

I. INTRODUCTION

WIRELESS power transfer based on magnetic resonance and near-field coupling of two loop resonators was first reported by Tesla in the 1880s [1]. Wireless power transfer can generally be classified as radiative and nonradiative. Radiative power transfer relies on high-frequency excitation of a power source, and radiative power is emitted from an antenna and propagates through a medium (such as vacuum or air) over long distance (i.e., many times larger than the dimension of the antenna) in the form of electromagnetic wave. Nonradiative wireless power transfer relies on the near-field electromagnetic coupling of conductive loops. Energy is transferred over a relatively short distance, which is on the order of the dimension (such as the radius or the diameter) of the coupled coils.

Manuscript received February 14, 2011; revised June 2, 2011 and August 10, 2011; accepted September 21, 2011. Date of publication October 10, 2011; date of current version September 6, 2012. This work was supported by the Hong Kong Research Grant Council under Project HKU-114410 and by The Hong Kong Polytechnic University under Project A-PK40.

W. X. Zhong is with the Centre for Power Electronics, Department of Electronic Engineering, City University of Hong Kong, Kowloon, Hong Kong (e-mail: wzhong3@student.cityu.edu.hk).

C. K. Lee is with the Department of Electrical Engineering, The Hong Kong Polytechnic University, Hung Hom, Hong Kong (e-mail: ecklee@polyu.edu.hk).

S. Y. R. Hui is with the Department of Electrical and Electronic Engineering, The University of Hong Kong, Pokfulam, Hong Kong, and also with the Department of Electrical and Electronic Engineering, Imperial College London, SW7 2AZ London, U.K. (e-mail: ronhui@eee.hku.hk; r.hui@imperial.ac.uk).

Color versions of one or more of the figures in this paper are available online at <http://ieeexplore.ieee.org>.

Digital Object Identifier 10.1109/TIE.2011.2171176

For efficient wireless power transfer, Tesla showed that using magnetic resonance of the coupled coils could achieve optimal energy transfer. In his experiment, Tesla used a conductive coil (which is the form of air-core inductor) connected in series with a Leyden jar (which is a form of capacitor) to form a loop resonator. He excited one loop (primary coil) as the power transmitter and used a second loop resonator (secondary coil) as a power receiver [2].

The same use of a pair of coupled coils for contactless power transfer [Fig. 1(a)] for short-range applications has attracted much interest in the last two decades. For example, research studies on wirelessly charging the batteries of mobile phones [3]–[11] and electric vehicles [12]–[15] usually use primary and secondary coils. For movable industrial robots used in production lines, the use of the power cable is a nuisance. The inductive power transfer systems for wirelessly charging industrial robots consist of primary and secondary coils coupled to each other [16]–[20], [31], [32]. The coils can be in the form of concentrated windings or spiral windings. For battery charging applications, the distance between the primary and secondary coils is usually smaller than the dimension of the primary and secondary coils. The ratio of transmission distance d and the radius of the coils r is less than three (i.e., $d/r < 3$). Such relatively short distance is termed “short-range” wireless power transfer. For very short-range applications such as wireless charging pads for mobile phones, such ratio can even be less than 1.0 in order to achieve high power transmission efficiency because the efficiency decreases rapidly with the transmission distance. For high-power applications of several kilowatts, the operating frequencies for wireless power transfer for electric vehicles and industrial robots are typically in several tens of kilohertz [16]–[20]. The primary and secondary circuits are usually resonant circuits in order to maximize power transfer efficiency—a principle set a century ago by Tesla. For “short-range” applications, typical transfer efficiency in the range of 80%–95% can be achieved.

The wireless power transfer experiment reported in [21] and [22] is essentially based on the magnetic coupling and resonance principles laid down by Tesla [1], [2]. Two coupled loop resonators (one transmitter and one receiver) are used in [21] and [22], and their emphasis is on the facts that a high Q factor is adopted and the distance d between the two coils is much greater than the dimension of the second coil (e.g., the radius r of a circular receiver coil), which is termed “mid-range” wireless power transfer for a ratio of $d/r > 3$. In order to enable a reasonable power transfer over “mid-range” distance, a high quality factor $Q = \omega L/R$ is needed, where $\omega = 2\pi f$ is the angular frequency, L is the inductance, and R is the resistance

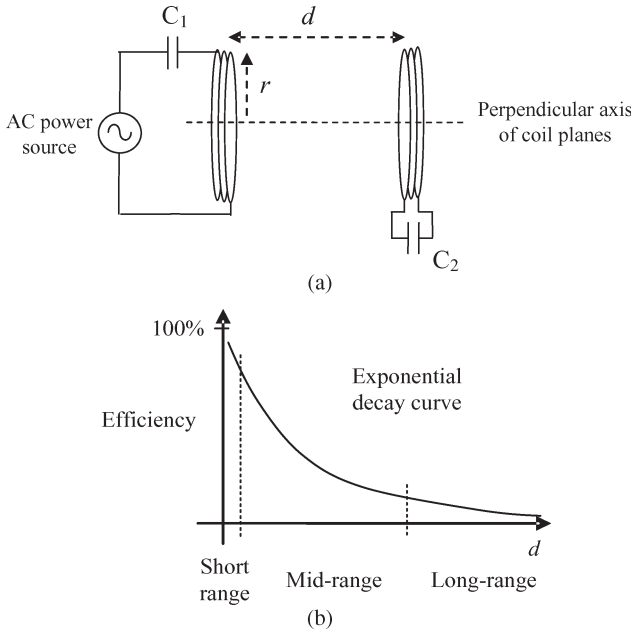


Fig. 1. (a) Pair of L - C loop resonators for wireless power transfer proposed by Tesla. (b) Typical exponential decay curve of the efficiency as a function of transmission distance d for wireless power transfer.

of the loop resonator at operating frequency f . To increase the transfer efficiency, an operating frequency of 10 MHz was adopted in [22]. For their system with a coil radius r of 30 cm, a transmission distance d of 2.4 m (i.e., a ratio of d/r of 8), and a Q of about 1000, an efficiency of 40% was reported.

Practical limitations of wireless power transfer have been addressed in [23] and [24]. If identical coils are used and $d \gg r$, it has been pointed out in [23] and [24] that the magnetic coupling coefficient and the efficiency will decrease rapidly with increasing transmission distance d . A typical graphical relationship of the power transmission efficiency versus transmission distance is shown in Fig. 1(b). In order to overcome the low efficiency for mid-range application, additional materials have been added between the transmitter and receiver coils. In [25], a metamaterial with a relative permeability equal to -1 is used to increase the transmission efficiency for a given distance. In [26], additional “relay” resonators are placed between the transmitter and receiver resonators in a domino arrangement in order to increase the efficiency effectively.

The use of the relay resonators has, in fact, been used previously in metamaterials and waveguide research. For example, magnetoinductive waveguide devices based on the use of a series of magnetically coupled LC loop resonators are set up in a chain with the loop planes perpendicular to an axis of wave propagation and with equal spacing between adjacent planes [27]–[29]. Generally, the dimensions of the coils and the separation distances are determined by the wavelength of the wave propagation. Since waveguides are designed for wave propagation and the operating frequencies are on the order of 100 MHz and above, such high-frequency operation inevitably increases the ac resistance of the coil resonators, which may limit their suitability for power transfer applications. However, the experience gained and basic principles obtained previously in the waveguide research do point to a viable solution to mid-

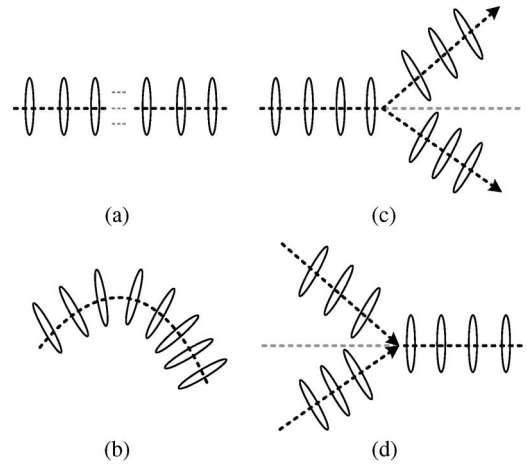


Fig. 2. Examples of the flexibility of the domino arrangements of resonators [26], [27]. (a) Straight chain. (b) Curved chain. (c) One chain splitting into two. (d) Two chains emerging into one.

range or even long-range wireless power transfer, particularly when such relay resonators can be flexibly arranged in various domino forms as suggested in [26]–[28] and as shown in Fig. 2.

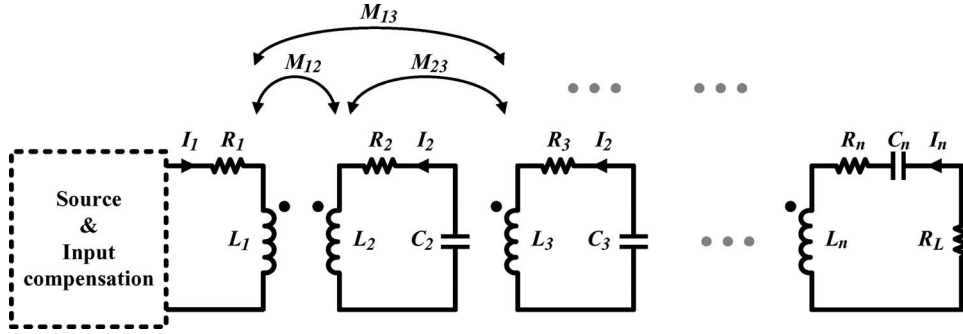
Since the Tesla experiment on near-field magnetic coupling is based on a pair of coil resonators, one main reason for its lack of application for mid- and long-range wireless power transfer is its low efficiency. Instead of using one excitation coil and one receiver coil, we investigate the use of several resonators [26]–[28] placed in or near the short-range region where the power transmission efficiency is high [Fig. 1(b)] in order to increase the overall transmission distance between the excitation power source and the load with reasonably high efficiency.

An analysis of the domino resonator arrangements for waveguide applications at 100 MHz has been reported in [29]. In [26], a straight domino of four resonators operating at 7 MHz for wirelessly powering an LED load is demonstrated. In this investigation, we present an analysis of the use of submegahertz operation (e.g., 520–530 kHz) for both coaxial and noncoaxial resonators in domino forms with the objectives of maximizing energy efficiency and increasing the transmission distance. Since the wavelength of such relatively low frequency exceeds 560 m while the power transmission distance is only a few meters, wireless power transfer occurs essentially via near-field magnetic coupling. Analytical equations for the optimal load and maximum efficiency are derived. We also propose simple power flow control methods and practically demonstrate that power flow can be controlled in domino resonators. Magnetically coupled resonators, each comprising a coil inductor connected in series with a capacitor, are arranged in various flexible domino arrangements (such as straight, curved, circular, and y-shaped) for evaluation.

II. ANALYSIS OF DOMINO RESONATORS

A. Circuit General Circuit Model and the Optimization Method

For a general (coaxial and noncoaxial) domino resonator system consisting of n coupled resonators shown in Fig. 3, the


 Fig. 3. Schematic of a system with n resonators.

general circuit equations can be expressed by (1), shown at the bottom of the page, where

$M_{ij} = k_{ij} \sqrt{L_i L_j}$ ($i, j = 1, 2, \dots, n; i \neq j$). Mutual inductance between windings i and j ;

R_L load resistance which is connected to winding n .

Other variables are

I_i current in winding i ;

L_i self-inductance of winding i ;

C_i compensating capacitance of winding i ;

R_i resistance in resonator i (including the resistance of winding i and the equivalent series resistance of capacitor C_i);

k_{ij} magnetic coupling coefficient between windings i and j ;

ω angular frequency.

Assuming that all coil resonators have the same resonance frequency, then $\omega L_i - 1/\omega C_i = 0$, $i = 2, 3, \dots, n$.

The efficiency of the n -winding system can be expressed as

$$\eta = \frac{I_n^2 R_L}{I_1^2 R_1 + I_2^2 R_2 + \dots + I_n^2 (R_n + R_L)} = \frac{R_L}{\left(\frac{I_1}{I_n}\right)^2 R_1 + \left(\frac{I_2}{I_n}\right)^2 R_2 + \dots + \left(\frac{I_{n-1}}{I_n}\right)^2 R_{n-1} + R_n + R_L}. \quad (2)$$

All of the terms I_m/I_n ($m = 1, 2, \dots, n-1$) in (2) can be worked out with (1). Thereby, the efficiency can be further expressed by a function

$$\eta = f(M_{12}, M_{13}, \dots, M_{(n-1)n}, R_1, R_2, \dots, R_n, R_L) \quad (3)$$

where the subscripts of mutual inductance M_{ij} refer to windings i and j .

1) *Mutual Inductance for Coaxial Resonators*: For two coaxial circular filamentary current loops, Maxwell [30] has derived a well-known equation to calculate the mutual inductance:

$$M = \mu_0 \frac{\sqrt{r_1 r_2}}{g} [(2 - g^2)K(g) - 2E(g)] \quad (4)$$

where $K(g)$ and $E(g)$ are complete elliptic integrals of the first and second kind, respectively, $\mu_0 = 4\pi \times 10^{-7}$ H/m, and

$$g = \sqrt{\frac{4r_1 r_2}{d^2 + (r_1 + r_2)^2}} \quad (5)$$

where r_1 , r_2 , and d are the radii of loop-1 and loop-2, and the distance between them, respectively.

For two coaxial circular thin-wall windings, if the dimension of the wire is relatively small compared to the dimension of the coils so that each turn of the windings can be considered as a filamentary current loop, then the mutual inductance between the two windings can be calculated by

$$M = \sum_{i=1}^{n_1} \sum_{j=1}^{n_2} M_{ij} \quad (6)$$

where n_1 and n_2 are the number of turns of the two windings and M_{ij} is the mutual inductance between the i turn of the first winding and the j turn of the second winding which can be worked out with (4).

Therefore, in a given domino resonator system with n coaxial circular windings, all mutual inductances between every two windings can be obtained using (4) and (6), and by substituting all the mutual inductances into (3), we can get the expression of efficiency as a function of the distances of every two adjacent windings and the load as

$$\eta = f(d_{12}, d_{23}, \dots, d_{(n-1)n}, R_L). \quad (7)$$

Then, with the total transmission distance given, the maximum efficiency and the optimum load, as well as the optimum distances between the resonators, can be obtained with the help of a numerical optimization tool such as MATLAB optimization toolbox.

$$\begin{bmatrix} j\omega M_{12} R_2 + j\left(\omega L_2 - \frac{1}{\omega C_2}\right) & j\omega M_{23} & \dots & \dots & j\omega M_{2n} \\ j\omega M_{13} & j\omega M_{23} R_3 + j\left(\omega L_3 - \frac{1}{\omega C_3}\right) & \dots & \dots & \dots \\ \vdots & \vdots & \vdots & \ddots & \vdots \\ j\omega M_{1(n-1)} & \dots & \dots & R_{n-1} + j\left(\omega L_{n-1} - \frac{1}{\omega C_{n-1}}\right) & j\omega M_{(n-1)n} \\ j\omega M_{1n} & \dots & \dots & j\omega M_{(n-1)n} & R_n + R_L + j\left(\omega L_n - \frac{1}{\omega C_n}\right) \end{bmatrix} \cdot \begin{bmatrix} \mathbf{I}_1 \\ \mathbf{I}_2 \\ \vdots \\ \mathbf{I}_{n-1} \\ \mathbf{I}_n \end{bmatrix} = 0 \quad (1)$$

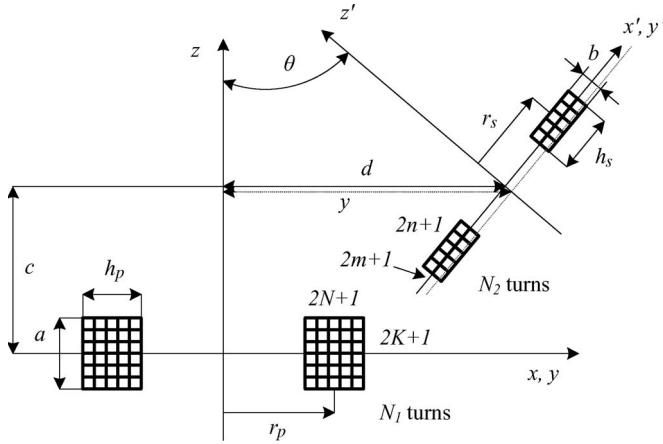


Fig. 4. Two noncoaxial circular coils [34].

2) *Mutual Inductance for Noncoaxial Resonators*: Based on the calculation method for the mutual inductance between two filamentary circular current loops with inclined axes in [33], the mutual inductance equation proposed in [34] for noncoaxial coils (see Fig. 4) is

$$M = \frac{N_1 N_2 \sum_{g=-K}^K \sum_{h=-N}^N \sum_{l=-n}^n \sum_{p=-m}^m M(g, h, l, p)}{(2K+1)(2N+1)(2n+1)(2m+1)} \quad (8)$$

where

$$M(g, h, l, p) = \frac{\mu_0}{\pi} \sqrt{r_p(h)r_s(l)} \int_0^\pi \frac{\left(\cos \theta - \frac{y(p)}{r_s(l)} \cos \phi \right) \Psi(g)}{V^{3/2}} d\phi$$

$$V = \sqrt{1 - \cos^2 \phi \sin^2 \theta - 2 \frac{y(p)}{r_s} \cos \phi \cos \theta + \frac{y^2(p)}{r_s^2}}$$

$$\Psi(g) = \left(\frac{2}{g} - g \right) K(g) - \frac{2}{g} E(g) = Q_{1/2}(x),$$

$$x = \frac{2 - g^2}{g^2}$$

$$y(p) = d + \frac{b \sin \theta}{2m+1} p, \quad p = -m, \dots, 0, \dots, m$$

$$r_p(h) = r_p + \frac{h_p}{2N+1} h, \quad h = -N, \dots, 0, \dots, N$$

$$r_s(l) = r_s + \frac{h_s}{2n+1} l, \quad l = -n, \dots, 0, \dots, n$$

$$z(g, p) = c + \frac{a}{2K+1} g - \frac{b \cos \theta}{2m+1} p,$$

$$g = -K, \dots, 0, \dots, K, \quad p = -m, \dots, 0, \dots, m$$

$$k^2 = \frac{4\alpha V}{(1 + \alpha V)^2 + \xi^2}, \quad \xi = \beta - \alpha \cos \phi \sin \theta,$$

$$\alpha = \frac{r_s}{r_p(h)},$$

$$\beta = \frac{z(g, p)}{r_p(h)}$$

r_p radius of the larger coil;
 h_p thickness of the larger coil;

a axial length of the larger coil;
 h_p thickness of the larger coil;
 a axial length of the larger coil;
 r_s radius of the smaller coil;
 h_s thickness of the smaller coil;
 b axial length of the smaller coil;
 c distance between coils' centers;
 d distance between coil planes;
 θ angle between axes;
 $K(g)$ complete elliptic integral of the first kind;
 $E(g)$ complete elliptic integral of the second kind;
 $Q_{1/2}(x)$ Legendre function of the second kind and half-integral degree.

B. Simplified Circuit Model

It should be stressed that the model (1) is a general model that includes the mutual inductance between adjacent coils and also the mutual inductance among nonadjacent coils. This means that (1) also includes the effects of the cross-coupling of nonadjacent coils. Due to the complexity of the cross-coupling among nonadjacent coils, it is not easy to derive analytical equation for optimization unless some assumptions are made. However, the model can be simplified in situation where the cross-coupling effects of nonadjacent coils can be neglected.

In the applications that the distances between every two adjacent resonators are relatively large (e.g., $d/r > 2$), the mutual inductance between every two nonadjacent resonators is negligibly small when compared with that between two adjacent resonators. The efficiency in (2) can be analytically determined by solving the simplified (1) in which all of the mutual inductances between two nonadjacent resonators are neglected.

Then, by solving the equation

$$\frac{\partial \eta}{\partial R_L} = 0 \quad (9)$$

we can get the analytical expressions for the optimum load and the maximum efficiency as follows

$$R_{L_OPT} = R_n \sqrt{\frac{\sum_{k=1}^n A_{k,n}^2 \delta_k}{\sum_{k=1}^{n-1} A_{k,n-1}^2 \delta_k}} \quad (10)$$

$$\eta_{max} = \frac{\delta_n}{2 \sqrt{\left(\sum_{k=1}^n A_{k,n}^2 \delta_k \right) \left(\sum_{k=1}^{n-1} A_{k,n-1}^2 \delta_k \right)} + 2 \sum_{k=1}^{n-1} A_{k,n} A_{k,n-1} \delta_k + \delta_n} \quad (11)$$

where

$$A_{k,n} = \sum_{E(k,n)} \left(\Delta_{(k+1)(k+2)}^{e(k+1)} \Delta_{(k+2)(k+3)}^{e(k+2)} \cdots \Delta_{(n-1)(n)}^{e(n-1)} \right)$$

for $k = 1, 2, \dots, n-2$ and $A_{n-1} = 1, A_n = 1$;

$$E(k, n) = \{ [e(k+1), e(k+2), \dots, e(n-1)] | e(m-1)e(m) \neq 1, m = k+1, \dots, n-2 \}$$

TABLE I
 PARAMETERS OF THE PRACTICAL RESONATORS

| | |
|-----------------------------|-----------------------------------|
| Radius of the winding | 155mm |
| Number of turns | 11 |
| Layers of the wire | 1 |
| Structure of the wire | Ø0.12mm×50strands Outer Ø1.2mm |
| Axial length of the winding | 15mm |
| Inductance (L) | 90.7µH |
| Capacitance (C) | 1nF |
| Resistance (at 530kHz) | 0.9Ω |
| Self-resonance frequency | 530kHz |

for $k = 1, 2, \dots, n - 2$;

$$e(k) \in \{0, 1\}, \quad \text{for } k = 2, 3, \dots, n - 1;$$

$$\delta_k = \prod_{g=1}^k \Delta_{(g-1)g}, \quad \text{for } k = 1, 2, \dots, n;$$

$$\Delta_{k(k+1)} = k_{k(k+1)}^2 Q_k Q_{k+1} = \frac{\omega^2 M_{k(k+1)}^2}{R_k R_{(k+1)}}$$

for $k = 1, 2, \dots, n - 1$ and $\Delta_{01} = 1$.

The optimum load and maximum efficiency can be obtained by (10) and (11) provided that all of the other parameters of the system have been given.

It should be noted that (10) and (11) provide a fast method for estimating the parameters for optimization of the energy efficiency, but they are only suitable for situations in which the mutual inductance between nonadjacent coils is negligible. In the following section on theoretical study, all of the theoretical results are obtained from the general model (1) that incorporates the cross-coupling effects.

III. THEORETICAL STUDY BASED ON PRACTICAL RESONATORS

A. Coaxial Domino Resonator Systems

Practical resonators have been built for various experiments. Theoretical studies have been conducted based on the parameters of the practical resonators, which are listed in Table I. The natural resonance frequency of the resonator can be calculated from

$$f_0 = 1/(2\pi\sqrt{LC}). \quad (12)$$

In this case, the nominal self-resonance frequency of the resonator is about 530 kHz.

1) *Equal-Spacing Arrangements of Coaxial (Straight) Dominos*: In the first theoretical study, adjacent resonators of the straight domino systems are placed 0.3 m apart. Tests are done with two resonators first and then progressively up to eight resonators. The accuracy of the simplified model is first checked with the general model. Efficiency of the simplified model is calculated with (11) and that for the general model with (1) using a numerical optimization method. The predictions of the energy efficiency for the Q factors of 1000 and 337 (i.e., practical value) are calculated and shown in Fig. 5. Their

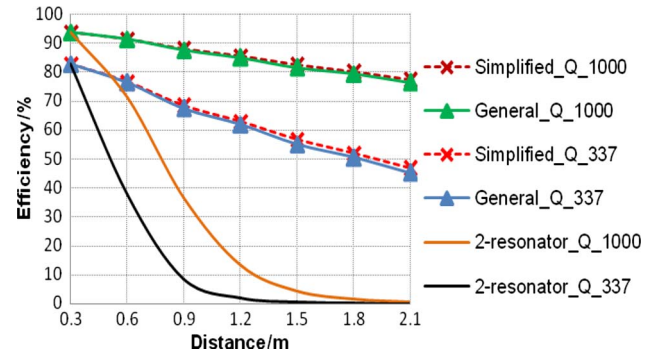


Fig. 5. Efficiency comparison between two-resonator and domino resonator with equal spacing.

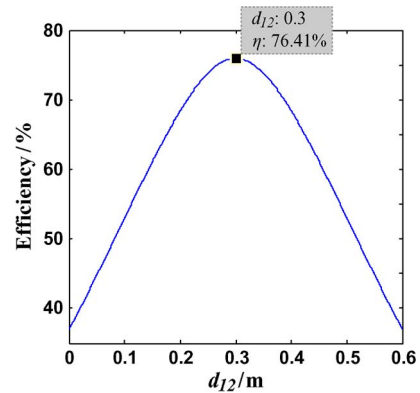


Fig. 6. Optimal spacing of a domino chain using three resonators for a total transmission distance of 0.6 m ($d_{\text{total}}/r = 3.87$). Equal-spacing arrangement offers best efficiency for a domino chain with three resonators.

efficiencies decrease linearly with transmission distance. It can be seen that the simplified and general models agree well in both cases and that the efficiency tends to decrease linearly with the transmission distance as the number of resonator increases.

The theoretical efficiency curves of a two-resonator system for the two Q factors are also shown in Fig. 5, and they exhibit exponential decay as expected. Comparison of the efficiency curve (linear decay) of the domino resonator arrangement and a two-resonator one clearly indicates the improvement of energy efficiency, as observed by the authors in [26].

2) *Optimum-Spacing Arrangements*: In the second theoretical study, MATLAB optimization toolbox is used to determine the spacing of the resonators for maximum energy efficiency. For a domino chain with three resonators, it can be shown in Fig. 6 that equal spacing of d_{12} and d_{23} offers the best efficiency. For the case of $n = 4$, the operating points of the optimum- and equal-spacing methods are highlighted in the 3-D efficiency plot in Fig. 7. Maximum efficiency occurs in a domino arrangement with unequal distances between the resonators, while equal spacing offers a near-optimal efficiency.

Our analysis shows that, when the number of resonators exceeds three, there exists an unequal-spacing arrangement [35] that offers the best efficiency, as shown in Fig. 8. In Fig. 8, the efficiency is calculated using the general model and a numerical optimization method. The optimum-spacing combinations for different distances are listed in Table II. Observations

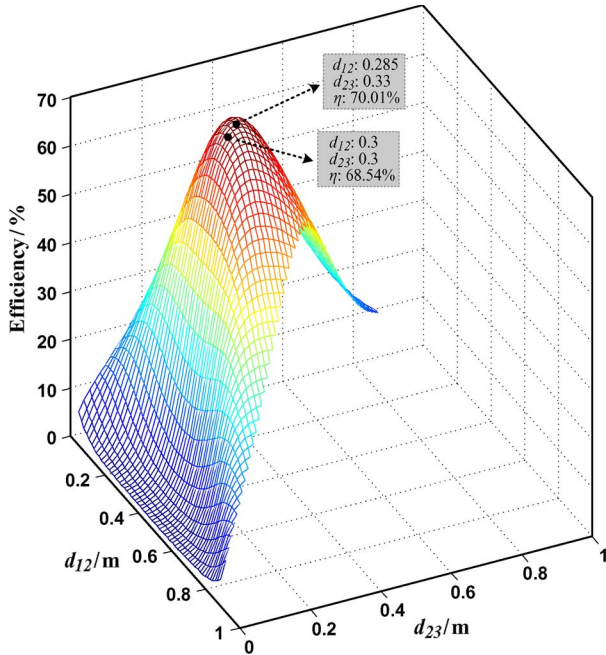


Fig. 7. Efficiency as a function of d_{12} and d_{23} for a system with four resonators.

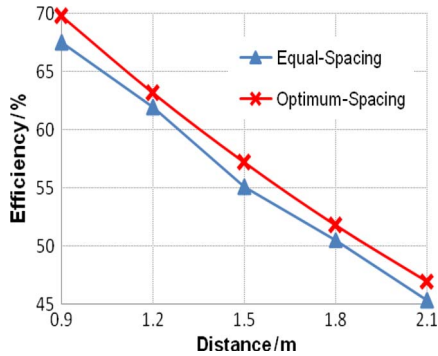


Fig. 8. Efficiency comparison between equal and optimum spacings for the domino resonator system with an average spacing of 0.3 m.

of the optimum-spacing values suggest the following for an n -resonator straight domino

- 1) Relay resonators (i.e., the second resonator to the $n - 1$ th resonator) can be essentially equally spaced. That is $d_{23} = \dots = d_{n-2,n-1} = d_{\text{relay}}$.
- 2) Distances between the transmitter (first) and second resonators, and the $n - 1$ th and receiver (n)th resonators can be the same. They should be smaller than the distance between adjacent relay resonators (i.e., $d_{12} = d_{n-1,n} < d_{\text{relay}}$).

These features can also be seen from the graphical representations in Fig. 9, which shows the ratios between optimum and average distances with different total transmission distances (i.e., different average distances d_A). This phenomenon might be explained by the fact that the relay resonators are magnetically coupled by two adjacent resonators while the transmitter and receiver resonators are coupled by only one adjacent resonator.

TABLE II
OPTIMUM-SPACING COMBINATIONS

| | <i>Optimum-spacing</i> | <i>Equal-spacing</i> |
|--|--|--|
| 4-resonator ($d_{\text{total}}=0.9\text{m}$) | $d_{12}=0.279\text{m}, d_{23}=0.341\text{m}, d_{34}=0.280\text{m},$ | $d_{12}=d_{23}=d_{34}=0.3\text{m}$ |
| 5-resonator ($d_{\text{total}}=1.2\text{m}$) | $d_{12}=0.269\text{m}, d_{23}=0.328\text{m}, d_{34}=0.333\text{m}, d_{45}=0.270\text{m}$ | $d_{12}=d_{23}=d_{34}=d_{45}=0.3\text{m}$ |
| 6-resonator ($d_{\text{total}}=1.5\text{m}$) | $d_{12}=0.262\text{m}, d_{23}=0.325\text{m}, d_{34}=0.324\text{m}, d_{45}=0.325\text{m}, d_{56}=0.264\text{m}$ | $d_{12}=d_{23}=d_{34}=d_{45}=d_{56}=0.3\text{m}$ |
| 7-resonator ($d_{\text{total}}=1.8\text{m}$) | $d_{12}=0.262\text{m}, d_{23}=0.316\text{m}, d_{34}=0.323\text{m}, d_{45}=0.318\text{m}, d_{56}=0.319\text{m}, d_{67}=0.262\text{m}$ | $d_{12}=d_{23}=d_{34}=d_{45}=d_{56}=d_{67}=0.3\text{m}$ |
| 8-resonator ($d_{\text{total}}=2.1\text{m}$) | $d_{12}=0.259\text{m}, d_{23}=0.318\text{m}, d_{34}=0.315\text{m}, d_{45}=0.317\text{m}, d_{56}=0.313\text{m}, d_{67}=0.317\text{m}, d_{78}=0.261\text{m}$ | $d_{12}=d_{23}=d_{34}=d_{45}=d_{56}=d_{67}=d_{78}=0.3\text{m}$ |

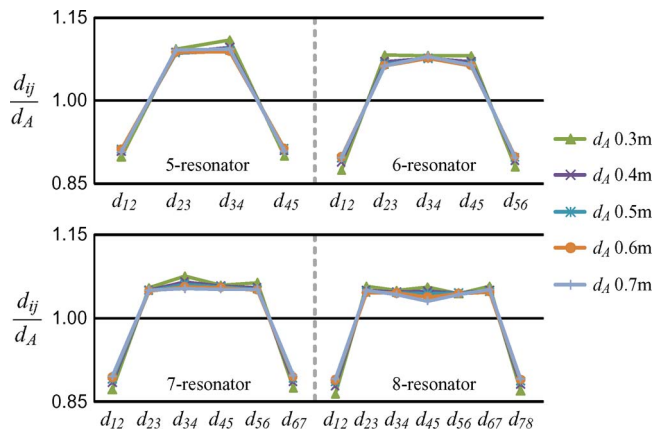


Fig. 9. Ratios between optimum and average distances with different total transmission distances (i.e., different average distances d_A).

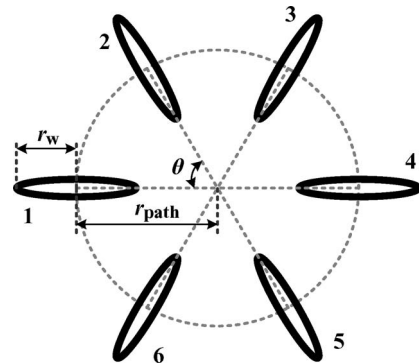


Fig. 10. Diagram of the equally spaced noncoaxial (circular) domino resonator system.

B. Noncoaxial Domino Resonator Systems

Without loss of generalization, a six-resonator circular domino system, as shown in Fig. 10, has been used as a case study example in order to check the validity of the general coupled circuit approach (1) and the equation for the noncoaxial resonators (8). Details of the spacial arrangement of the six resonators and their parameters are included in Table III. Unlike the tests for the coaxial resonator system previously described, a different set of capacitors is used in this noncoaxial resonator

TABLE III
 PARAMETERS OF THE CIRCULAR DOMINO RESONATOR SYSTEM

| | |
|--------------------------|--------------|
| Number of resonators | 6 |
| Transmitter resonator | Resonator-1 |
| L | 90.7 μ H |
| C | 1.034 nF |
| R | 0.9 Ω |
| Receiver resonator | Resonator-4 |
| r_{path} | 0.3 m |
| r_w | 0.155 m |
| θ | 60 $^\circ$ |
| Load | 17 Ω |
| Self-resonance frequency | 520 kHz |

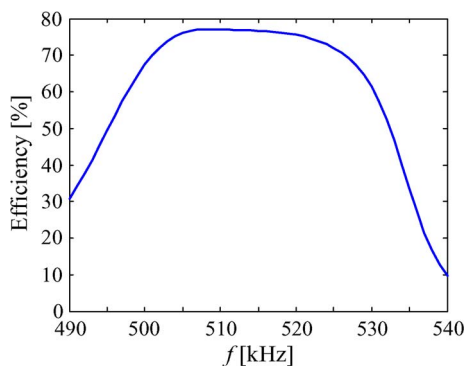


Fig. 11. Theoretical energy efficiency as a function of the operating frequency.

tests. The nominal self-resonance frequency is 520 kHz instead of 530 kHz.

Based on the general model (1) and the parameters in Table III for this circular domino resonator system, the theoretical efficiency curve is plotted against the operating frequency in Fig. 11. In the theoretical study, resonator-1 is the transmitter, and resonator-4 is the receiver, which is loaded with a resistor. It is noted that an energy efficiency exceeding 75% is expected from this practical system in the frequency range of 505–525 kHz.

IV. PRACTICAL VERIFICATION

An amplifier research RF power amplifier (Model 75A250A) is used to drive the domino systems in this paper. For the tests using resistive loads (Sections IV-A and IV-B), the load power is tested to typically 10 W. However, for practical demonstrations using lighting devices (Section IV-C), power up to about 30 W is transferred wirelessly.

A. Domino Resonator in Coaxial (Straight) Arrangement

Practical verifications of the analysis have been performed using the resonators specified in Table I. The operation frequency is set at a nominal resonance frequency, which is about 530 kHz. The output and input power values are measured using high-speed high-storage digital oscilloscope Tektronix DPO 7104. The sampling rate is set at 5G samples per second, and over 50 cycles of the sampled voltage and current waveforms are used to derive the average power values.

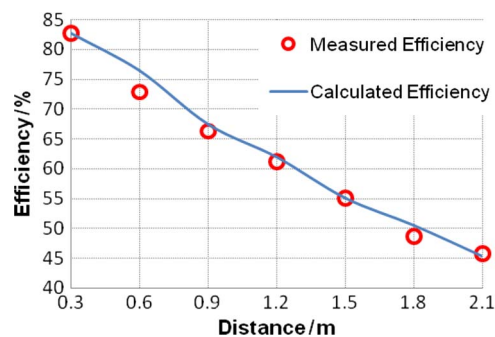


Fig. 12. Measured and calculated efficiencies of the equal-spacing domino resonator systems.

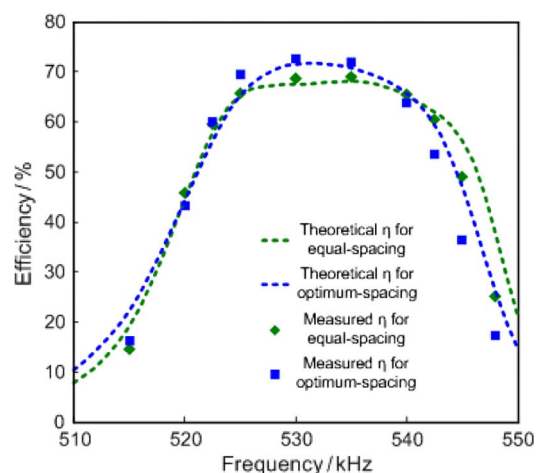


Fig. 13. Theoretical and measured efficiencies of four resonators arranged in a straight domino form.

The efficiency of the equally spaced domino resonator systems is first checked and recorded in Fig. 12. Experimental results are in good agreement with the theoretical values, which proves that the efficiency of the domino resonator system decreases almost linearly with the transmission distance.

In order to evaluate the efficiency of the equal- and optimum-spacing approaches more closely, tests are conducted by scanning the frequency around the resonant point for a four-resonator system. The transmission distance is 0.9 m, and the optimum spacing is $d_{12} = 0.28$ m, $d_{23} = 0.34$ m, and $d_{34} = 0.28$ m, as shown in Table II. The theoretical and measured results are shown in Fig. 13. It can be seen that the energy efficiency of the optimum-spacing arrangement is slightly higher than that of the equal-spacing one in this paper. The measurements are generally in agreement with the theoretical ones.

It should be noted that, in the theoretical analysis in Section III, the optimum arrangements are based on the identical resonators. If the parameters of the practical resonators have a large tolerance (e.g., 10%), the optimum spacing will be affected, and thereby, it will be different from the theoretical values. Considering the difficulty of building resonators with very small tolerance in laboratory, it would be difficult to differentiate the small efficiency difference in experiments for the optimum spacing of the domino resonator systems with a large number of resonators because the parameter variations

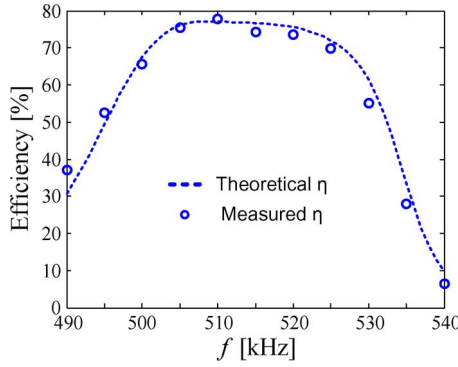


Fig. 14. Measured and theoretical energy efficiencies.

of the resonators could mask the small efficiency difference between optimum- and equal-spacing methods. For the tests on the four-resonator system with results recorded in Fig. 13, four resonators are carefully chosen so that their parameters are within a relatively small tolerance of 3%.

B. Resonators in Circular Domino Arrangements

The circular domino resonator system based on the use of six resonators in Fig. 10 and the parameters of Table III has been practically evaluated. With resonator-1 excited by an RF power amplifier and resonator loaded with a resistor, tests are conducted to drive the load to about 10 W. The energy efficiency of the system over a range of frequency is measured and shown with the theoretical values in Fig. 14. The measurements confirm the validity of the general model and the mutual inductance for noncoaxial coils.

C. Resonators in Other Domino Arrangements

The use of domino arrangements of the loop resonators [26], [27] enables the control of the power in a highly flexible manner. Straight, curved, circular, and even irregularly shaped domino paths can easily be formed to direct the power flow. A power flow path can be split into two paths, which can, in turn, merge into a single path. Power flow control can be achieved by altering the impedance of the power flow paths [35] via the following: 1) the angle of the coil plane of the resonators [Fig. 15(a)] and 2) detuning the resonance frequency of the resonators [Fig. 15(b)]. Detuning the resonance frequency for power flow control in wireless applications has been reported in [36] and [37] in which a parallel variable inductor is used to alter the resonance frequency. However, for domino resonator applications, it is easier to alter the resonant capacitor values than changing the number of turns in each resonator coil [37]. Switched capacitor circuits can be used to change the capacitance and, thus, the impedance and resonance frequency of the resonators.

Fig. 16 shows ten resonators arranged in straight coaxial domino of 3 m with a d_{total}/r ratio equal to 19.4 (i.e., $3/0.155$) and a load of four 8-W LEDs. Fig. 17(a) shows a noncoaxial domino resonator system with one power flow path bending 90° and then splitting into two paths, each loaded with four

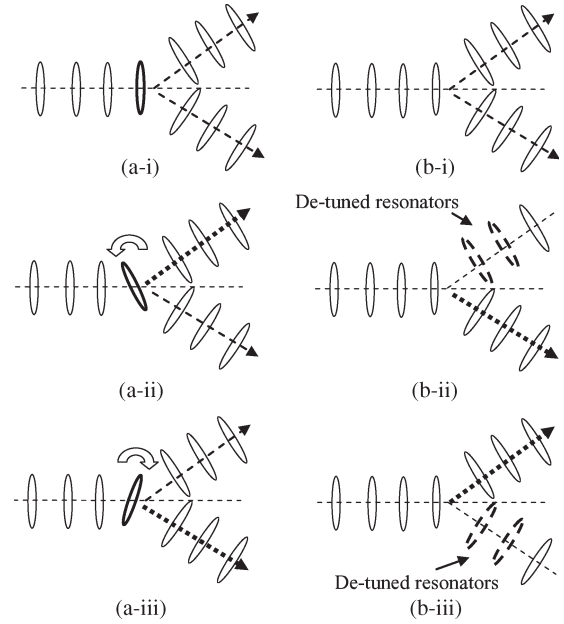


Fig. 15. Proposed power flow control methods by (a) angle control of the loop plane and (b) resonance frequency/impedance control of loop resonators.



Fig. 16. Straight coaxial domino chain of 3 m and a load of four 8-W LEDs (d_{total}/r ratio = 19.4).

8-W LEDs. Fig. 17(b) shows a photograph of the system in Fig. 15(a) using the angle control of the resonator to channel more power to the LED load at the left. A circular domino arrangement powering a 14-W compact fluorescent lamp is shown in Fig. 18.

V. CONCLUSION

Based on the experience gained in the century-old Tesla's magnetically coupled resonator experiment, the magnetoinductive resonator techniques used in previous waveguide design, and the relay resonator concept, we have demonstrated the flexibility of using magnetically coupled resonators in various domino forms for wireless power transfer and have proposed simple techniques for power flow control. Using the general coupled circuit modeling technique that incorporates mutual

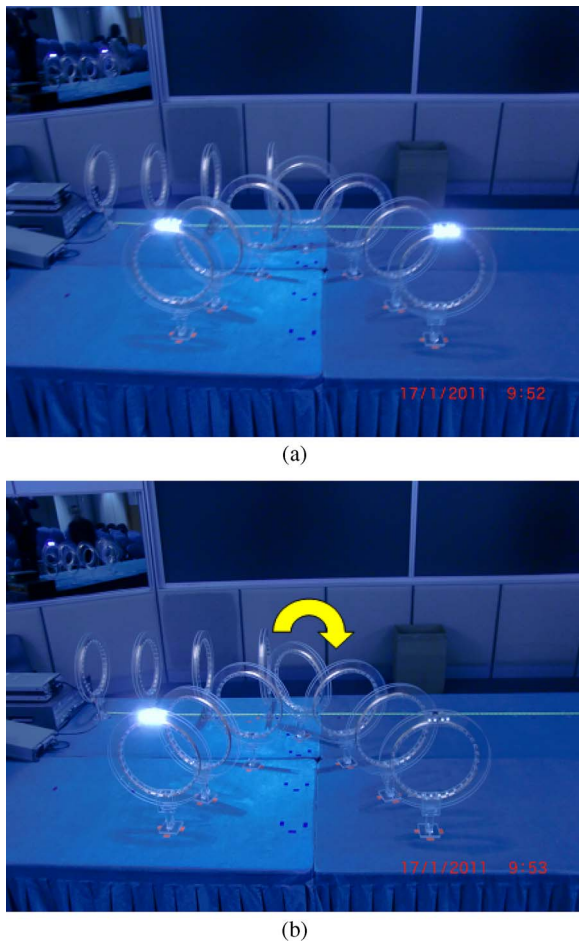


Fig. 17. (a) Domino resonator system with the power flow path bending 90° and then splitting into two paths, each loaded with four 8-W LEDs. (b) Photograph of the domino resonator system of Fig. 11(a) using angle control to channel more power to the LED load at the left.

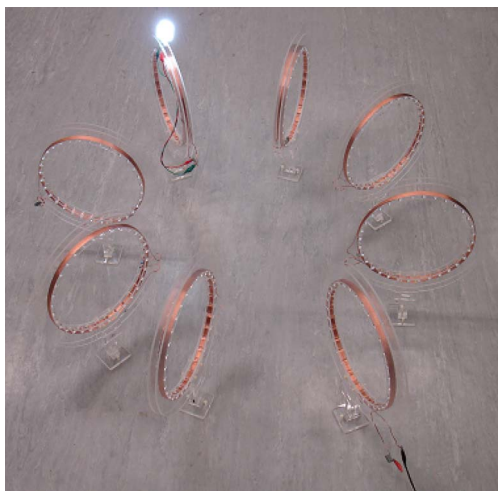


Fig. 18. Circular domino resonator system powering a 14-W compact fluorescent lamp.

inductance between adjacent resonators and among nonadjacent resonators, both coaxial and noncoaxial domino resonator systems have been successfully modeled with great accuracy as confirmed by the practical measurements.

It is possible to use submegahertz operation for wireless power transfer. Such technique allows the switching losses in the power electronic driving circuit and the resonator's winding loss (due to frequency-dependent skin effects) to be reduced. Besides reconfirming previous research finding that the relay resonators can substantially increase the overall wireless power transfer distance while achieving reasonably high efficiency, we have proposed an optimization method for domino resonator systems based on the general circuit model and the use of a numerical optimization tool.

For the straight coaxial domino resonator system, it is discovered that unequal-spacing arrangement works better than equal-spacing one. In particular, the spacing between the first two resonators and that between the last two resonators of the straight domino system should be smaller than the distance between the relay resonators. The optimum results have been practically verified. Also, analytical expressions have been successfully derived for the optimal load and the maximum efficiency at resonance operation for domino resonator systems based on the simplified circuit model. These analytical equations can be used for further study on the optimum operation of the domino resonator systems.

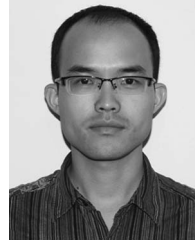
ACKNOWLEDGMENT

The authors would like to thank W. H. Mak for his help in constructing the resonators.

REFERENCES

- [1] H. W. Secor, "Tesla apparatus and experiments—How to build both large and small Tesla and Oudin coils and how to carry on spectacular experiments with them," *Practical Electricians*, Nov. 1921.
- [2] R. Lomas, *The Man Who Invented the Twentieth Century—Nikola Tesla—Forgotten Genius of Electricity*. London, U.K.: Headline, 1999, p. 146.
- [3] K. Oguri, "Power supply coupler for battery charger," U.S. Patent 6 356 049, Mar. 12, 2002.
- [4] Y. Yang and M. Jovanovic, "Contactless electrical energy transmission system," U.S. Patent 6 301 128, Oct. 9, 2001.
- [5] H. J. Brockmann and H. Turtiainen, "Charger with inductive power transmission for batteries in a mobile electrical device," U.S. Patent 6 118 249, Sep. 12, 2000.
- [6] B. Choi, J. Nho, H. Cha, T. Ahn, and S. Choi, "Design and implementation of low-profile contactless battery charger using planar printed circuit board windings as energy transfer device," *IEEE Trans. Ind. Electron.*, vol. 51, no. 1, pp. 140–147, Feb. 2004.
- [7] Y. Jang and M. M. Jovanovic, "A contactless electrical energy transmission system for portable-telephone battery chargers," *IEEE Trans. Ind. Electron.*, vol. 50, no. 3, pp. 520–527, Jun. 2003.
- [8] C.-G. Kim, D.-H. Seo, J.-S. You, J.-H. Park, and B. H. Cho, "Design of a contactless battery charger for cellular phone," *IEEE Trans. Ind. Electron.*, vol. 48, no. 6, pp. 1238–1247, Dec. 2001.
- [9] S. Y. R. Hui and W. C. Ho, "A new generation of universal contactless battery charging platform for portable consumer electronic equipment," *IEEE Trans. Power Electron.*, vol. 20, no. 3, pp. 620–627, May 2005.
- [10] X. Liu and S. Y. R. Hui, "Simulation study and experimental verification of a contactless battery charging platform with localized charging features," *IEEE Trans. Power Electron.*, vol. 22, no. 6, pp. 2202–2210, Nov. 2007.
- [11] S. Y. R. Hui, "Planar inductive battery charging system," U.S. Patent 7 576 514, Aug. 18, 2009.
- [12] A. Esser, "Contactless charging and communication for electric vehicles," *IEEE Ind. Appl. Mag.*, vol. 1, no. 6, pp. 4–11, Nov./Dec. 1995.
- [13] T. Imura, H. Okabe, and Y. Hori, "Basic experimental study on helical antennas of wireless power transfer for electric vehicles by using magnetic resonant couplings," in *Proc. IEEE VPPC*, 2009, pp. 936–940.

- [14] Y. Hori, "Future vehicle society based on electric motor, capacitor and wireless power supply," in *Proc. IPEC*, 2010, pp. 2930–2934.
- [15] K. Sugimori and H. Nishimura, "A novel contact-less battery charger for electric vehicles," in *Proc. 29th Annu. IEEE Power Electron. Spec. Conf.*, 1998, vol. 1, pp. 559–564.
- [16] H. H. Wu, J. T. Boys, and G. A. Covic, "An ac processing pickup for IPT systems," *IEEE Trans. Power Electron.*, vol. 25, no. 5, pp. 1275–1284, May 2010.
- [17] H. L. Li, A. P. Hu, G. A. Covic, and C. S. Tang, "Optimal coupling condition of IPT system for achieving maximum power transfer," *Electron. Lett.*, vol. 45, no. 1, pp. 76–77, Jan. 2009.
- [18] A. P. Hu, C. Liu, and H. L. Li, "A novel contactless battery charging system for soccer playing robot," in *Proc. 15th Int. Conf. Mechatronics Mach. Vis. Pract.*, 2008, pp. 646–650.
- [19] G. A. Covic, J. T. Boys, M. L. G. Kissin, and H. G. Lu, "A three-phase inductive power transfer system for roadway-powered vehicles," *IEEE Trans. Ind. Electron.*, vol. 54, no. 6, pp. 3370–3378, Dec. 2007.
- [20] Z. Pantic, S. Bhattacharya, and S. Lukic, "Optimal resonant tank design considerations for primary track compensation in inductive power transfer systems," in *Proc. IEEE ECCE*, 2010, pp. 1602–1609.
- [21] A. Karalis, A. B. Kurs, R. Moffatt, J. D. Joannopoulos, P. H. Fisher, and M. Soljacic, "Wireless energy transfer," U.S. Patent 7825 543B2, Nov. 2, 2010.
- [22] A. Kurs, A. Karalis, R. Moffatt, J. D. Joannopoulos, P. Fisher, and M. Soljacic, "Wireless power transfer via strongly coupled magnetic resonances," *Science*, vol. 317, no. 5834, pp. 83–86, Jul. 6, 2007.
- [23] E. Waffenschmidt and T. Staring, "Limitation of inductive power transfer for consumer applications," in *Proc. Eur. Conf. Power Electron. Appl., EPE*, 2009, pp. 1–10.
- [24] J. O. Mur-Miranda, G. Fantì, Y. Feng, K. Omanakuttan, R. Ongie, A. Setjoadi, and N. Sharpe, "Wireless power transfer using weakly coupled magnetostatic resonators," in *Proc. IEEE ECCE Conf.*, 2010, pp. 4179–4186.
- [25] J. Choi and C. Seo, "High-efficiency wireless energy transmission using magnetic resonance based on metamaterial with relative permeability equal to -1 ," *Prog. Electromagn. Res.*, vol. 106, pp. 33–47, 2010.
- [26] F. Zhang, S. Hackworth, W. Fu, and M. Sun, "The relay effect on wireless power transfer using wtricity," in *Proc. IEEE Conf. Electromagn. Field Comput.*, Chicago, IL, May 9–12, 2010.
- [27] R. Syms, E. Shamonina, and L. Solymar, "Magneto-inductive waveguide devices," *Proc. Inst. Elect. Eng.—Microw., Antennas Propag.*, vol. 153, no. 2, pp. 111–121, Apr. 2006.
- [28] R. Syms, E. Shamonina, V. Kalinin, and L. Solymar, "A theory of metamaterials based on periodically loaded transmission lines: Interaction between magnetoinductive and electromagnetic waves," *J. Appl. Phys.*, vol. 97, no. 6, p. 064909, Mar. 2005.
- [29] R. Syms, L. Solymar, I. R. Young, and T. Floume, "Thin-film magneto-inductive cables," *J. Phys. D, Appl. Phys.*, vol. 43, no. 5, p. 055 102, Feb. 2010.
- [30] J. C. Maxwell, *A Treatise on Electricity and Magnetism*. New York: Dover, 1954.
- [31] N. A. Keeling, G. A. Covic, and J. T. Boys, "A unity-power-factor IPT pickup for high-power applications," *IEEE Trans. Ind. Electron.*, vol. 57, no. 2, pp. 744–751, Feb. 2010.
- [32] M. L. G. Kissin, J. T. Boys, and G. A. Covic, "Interphase mutual inductance in polyphase inductive power transfer systems," *IEEE Trans. Ind. Electron.*, vol. 56, no. 7, pp. 2393–2400, Jul. 2009.
- [33] F. W. Grover, *Inductance Calculations*. New York: Dover, 1964.
- [34] S. I. Babic and C. Akyel, "Calculating mutual inductance between circular coils with inclined axes in air," *IEEE Trans. Magn.*, vol. 44, no. 7, pp. 1743–1750, Jul. 2008.
- [35] S. Y. R. Hui and W. X. Zhong, "Apparatus and method for wireless power transfer," Patent application PCT/IB2011/000050, Jan. 14, 2011.
- [36] A. P. Hu and S. Hussmann, "Improved power flow control for contactless moving sensor applications," *IEEE Power Electron. Lett.*, vol. 2, no. 4, pp. 135–138, Dec. 2004.
- [37] P. Si, A. P. Hu, S. Malpas, and D. Budgett, "Switching frequency analysis of dynamically detuned ICPT power pick-ups," in *Proc. Int. Conf. Power Syst. Technol.*, Chongqing, China, 2006, pp. 1–8.



Wenxing Zhong was born in China in 1984. He received the B.S. degree in electrical engineering from Tsinghua University, Beijing, China, in 2007. He is currently working toward the Ph.D. degree in the Centre for Power Electronics, City University of Hong Kong, Kowloon, Hong Kong.

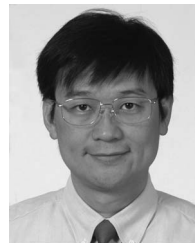
His current research interests include synchronous rectification and wireless power transfer.



Chi Kwan Lee (M'08) received the B.Eng. and Ph.D. degrees in electronic engineering from the City University of Hong Kong (CityU), Kowloon, Hong Kong, in 1999 and 2004, respectively.

He was a Postdoctoral Research Fellow with the Power and Energy Research Centre, National University of Ireland, Galway, Ireland, from 2004 to 2005. In 2006, he joined the Centre for Power Electronics, CityU, as a Research Fellow. He is currently a Lecturer with the Department of Electrical Engineering, The Hong Kong Polytechnic University,

Hung Hom, Hong Kong. His current research interests include applications of power electronics to power systems, advanced inverters for renewable energy and smart grid applications, reactive power control for load management in renewable energy systems, wireless power transfer, energy harvesting, and planar electromagnetics for high-frequency power converters.



S. Y. Ron Hui (F'03) received the B.Sc.Eng. degree (Hons.) from the University of Birmingham, Birmingham, U.K., in 1984 and the D.I.C. and Ph.D. degrees from Imperial College London, London, U.K., in 1987.

He has previously held academic positions at the University of Nottingham, Nottingham, U.K., from 1987 to 1990, University of Technology Sydney, Sydney, Australia, from 1991 to 1992, University of Sydney, Sydney, from 1992 to 1996, and City University of Hong Kong (CityU), Kowloon, Hong

Kong, from 1996 to 2011. Since July 2011, he has held the Chair Professorship at The University of Hong Kong, Pokfulam, Hong Kong. Since July 2010, he has concurrently held the Chair Professorship at the Imperial College London. He has published over 200 technical papers, including more than 150 refereed journal publications and book chapters. Over 50 of his patents have been adopted by industry.

Dr. Hui is a Fellow of the Institution of Engineering & Technology. He has been an Associate Editor of the IEEE TRANSACTIONS ON POWER ELECTRONICS since 1997 and an Associate Editor of the IEEE TRANSACTIONS ON INDUSTRIAL ELECTRONICS since 2007. He was appointed twice as an IEEE Distinguished Lecturer by the IEEE Power Electronics Society in 2004 and 2006. He served as one of the 18 Administrative Committee members of the IEEE Power Electronics Society and was the Chairman of its Constitution and Bylaws Committee from 2002 to 2010. He received the Excellent Teaching Award at CityU in 1998 and the Earth Champion Award in 2008. He won an IEEE Best Paper Award from the IEEE IAS Committee on Production and Applications of Light in 2002 and two IEEE Power Electronics Transactions Prize Paper Awards for his publications on wireless charging platform technology in 2009 and on LED system theory in 2010. His inventions on wireless charging platform technology underpin key dimensions of Qi, the world's first wireless power standard, with freedom of positioning and localized charging features for wireless charging of consumer electronics. In November 2010, he received the IEEE Rudolf Chope R&D Award from the IEEE Industrial Electronics Society and the IET Achievement Medal (The Crompton Medal) and was elected to the Fellowship of the Australian Academy of Technological Sciences & Engineering.